# Accumulation of Actin in Subsets of Pioneer Growth Cone Filopodia in Response to Neural and Epithelial Guidance Cues In Situ

**Timothy P. O'Connor and David Bentley**

Division of Neurobiology, Department of Molecular and Cell Biology, University of California, Berkeley, California 94720

*Abstract.* Directed outgrowth of neural processes must involve transmission of signals from the tips of filopodia to the central region of the growth cone. Here, we report on the distribution and dynamics of one possible element in this process, actin, in live growth cones which are reorienting in response to in situ guidance cues. In grasshopper embryonic limbs, pioneer growth cones respond to at least three types of guidance cues: a limb axis cue, intermediate target cells, and a circumferential band of epithelial cells. With time-lapse imaging of intracellularly injected rhodamine–phalloidin and rhodamine–actin, we monitored the distribution of actin during growth cone responses to these cues. In distal limb regions, accumulation of actin in filopodia and growth cone branches accompanies continued growth, while reduction of actin accompanies withdrawal. Where growth cones are reorienting to intermediate target cells, or along the circumferential epithelial band, actin selectively accumulates in the proximal regions of those filopodia that have contacted target cells or are extending along the band. Actin accumulations can be retrogradely transported along filopodia, and can extend into the central region of the growth cone. These results suggest that regulation and translocation of actin may be a significant element in growth cone steering.

During development of the nervous system, the establishment of correct connectivity is based in part upon the ability of extending nerve fibers to be directed by extracellular guidance information. Interactions between the molecules that constitute guidance information and receptors on the growth cone surface must transmit signals to the interior of the growth cone that locally effect the organization and consolidation of the cytoskeleton (Mitchison and Kirschner, 1988). In the results reported here, we have used time-lapse imaging to monitor the distribution of one cytoskeletal element, actin, during migration and turning of growth cones in response to their normal, in situ, guidance cues.

The interfaces between an extending nerve fiber and its embryonic environment are the leading edges of filopodia and lamellipodia that protrude from the growth cone. Filopodia are tubular actin-based structures (Letourneau, 1983; Bridgman and Dailey, 1989), whose core is a bundle of 15 or more actin filaments (Lewis and Bridgman, 1992). The filaments, comprised of two strands of polymer arranged in an $\alpha$-helix, are polarized, with their barbed ends usually oriented distally in the filopodium (Pollard, 1990; Cooper, 1991, Lewis and Bridgman, 1992). Immuno-electron microscopy, photo-bleaching, photo-activation, and high-resolution video-imaging in combination with cytochalasin treatment, show that actin filaments polymerize at the tips of filopodia and at the leading edges of lamellipodia (Wang, 1985; Forscher and Smith, 1988; Smith, 1988; Okabe and Hirokawa, 1989, 1991; Theriot and Mitchison, 1992*a*, *b*), and are retrogradely transported toward the central region of the growth cone. Some actin filament bundles have been observed to extend into the central region of the growth cone (Letourneau, 1983; Bridgman and Dailey, 1989; Lewis and Bridgman, 1992) and even to enter the nascent axon (Gordon-Weeks, 1987), while others predominantly terminate at the transition between the peripheral domain and the central domain (Forscher and Smith, 1988). Measurements of actin filament stability in the lamellae of fibroblasts and keratocytes suggest that many short, cross-linked actin filaments are moving as a unit, and undergo rapid turnover (Theriot and Mitchison, 1992*a*,*b*).

To investigate the distribution of actin during growth cone migration and turning, we studied Til pioneer growth cones migrating in grasshopper embryo limb buds (Bate, 1976; Bentley and O'Connor, 1992). The pair of sibling Til neurons arise from a mother cell at the tip of the limb bud at 30% of embryogenesis and extend axons proximally through

Address all correspondence to Dr. T. P. O'Connor, Life Sciences Addition, Department of Molecular and Cell Biology, University of California, Berkeley, CA 94720.

© The Rockefeller University Press, 0021-9525/93/11/935/14 $2.00

the limb along a stereotyped route to the CNS (see Fig. 1). The growth cones migrate between the basal lamina and the basal surfaces of the epithelial cells (Anderson and Tucker, 1988). Although growth cones normally adhere to the basal lamina, microdissection and enzymatic treatment experiments have shown that adequate guidance information can be provided by the epithelium and a small set of pre-axonogenesis neurons, termed guidepost cells, derived from it (Lefcort and Bentley, 1987; Condic and Bentley, 1989*a*, *b*). The pioneer growth cones and the guidepost cells both express, fasciclin I (Bastiani et al., 1987), a glycosylphosphatidylinositol (GPI)[1]-anchored homophilic adhesion protein (Elkins et al., 1990), that appears to mediate fasciculation between the two Til axons (Jay and Keshishian, 1990), as well as lachesin, a GPI-anchored member of the immunoglobin superfamily (Karlstrom et al., 1993). Treatment of limbs with phosphatidylinositol-specific phospholipase C, which should remove fasciclin I, lachesin, and other GPI-anchored molecules, disrupts guidance (Chang et al., 1992). The limb epithelium is partitioned into a set of segmentally iterated, circumferential bands that express different membrane-associated molecules. A distal band in each limb segment expresses annulin, a putative membrane-associated transglutaminase (Bastiani et al., 1992; Singer et al., 1992) and, in cockroach embryos, the DSS-8 antigen, a 164-kD transmembrane glycoprotein (Norbeck and Denburg, 1991). An intrasegmental band expresses fasciclin IV (Kolodkin et al., 1992), a transmembrane glycoprotein, and an intersegmental band expresses epithelial alkaline phosphatase, another GPI-anchored molecule (Chang et al., 1993). Fasciclin IV has been shown to be necessary for normal guidance. Finally, at least three distal–proximal molecular gradients are expressed during Til pioneer growth cone migration in embryonic cockroach limb buds (Norbeck et al., 1992). They may mediate guidance, possibly involving proteoglycans (Wang and Denburg, 1992), along the limb axis.

Til pioneer growth cones project numerous lengthy filopodia which typically extend 30 $\mu$m or more from the growth cone (Caudy and Bentley, 1986). These filopodia are not required for growth cone migration, but are required for normal guidance (Bentley and Toroian-Raymond, 1986). Videoimaging of growth cones labeled with lipophilic fluorescent dyes during migration on the limb epithelium shows that the form of the growth cone during migration and turning varies considerably, depending upon the limb region being traversed (O'Connor et al., 1990). At some locations growth cones turn by dilation of a single filopodium which has contacted a high affinity substrate. Similar filopodial dilation turning events have been described in grasshopper (Myers and Bastiani, 1993), and mammalian (Mason and Godement, 1992) central nervous systems (CNSs). During migration and turning, the disposition and behavior of microtubules has been imaged in live Til growth cones by intracellular injection of rhodaminated bovine tubulin (Sabry et al., 1991). Depending upon the limb region being traversed, microtubule disposition within the growth cone can become restricted to one location either by selective retention of microtubules in branches that have been extended in the preferred direction, or by selective intrusion of microtubules into a branch forming from a dilating filopodium. Particularly in the latter case, it is clear that the branch dilates in advance of microtubule intrusion, rather than being caused to dilate by the arrival of microtubules. The clear existence of this earlier morphological event in filopodial dilation motivated our examination of actin distribution during growth cone turning.

1. *Abbreviations used in this paper*: CNS, central nervous system; GPI, glycosylphosphatidylinositol; r-phalloidin, rhodamine-phalloidin; r-actin, rhodaminated actin.

## Materials and Methods

### Actin Preparation and Fluorescent Labeling

Actin was prepared from rabbit muscle acetone powder (Sigma Chemical Co., St. Louis, MO) as outlined by Pardee and Spudich (1982). Briefly, G-actin was extracted by adding five grams of acetone powder to 100 ml of G buffer (G buffer; 5 mM Tris-HCl pH 8.0, 0.2 mM $CaCl_2$, 0.2 mM ATP, 0.2 mM DTT) and stirring for 30 min at 4°C. The solution of hydrated powder was filtered through several layers of cheesecloth. The solid residue was resuspended in 50 ml of G buffer and filtered a second time. The filtrates were combined and centrifuged in a SA-600 rotor at 10,000 rpm for 1 h at 4°C. After discarding the supernatant, the G-actin was polymerized by adding F buffer (F buffer, final concentration: 1 mM ATP, pH 8.0, 2 mM $MgCl_2$, and 50 mM KCl), covered and left at 4°C for 2 h. To remove tropomyosin, solid KCl was slowly added to a final concentration of 0.6 M KCl, and the solution was stirred vigorously for 1 h at 4°C. F-actin was retrieved by centrifuging for 1.5 h at 40,000 rpm in a 50.2 Ti rotor at 4°C. The pellet was homogenized and resuspended in G buffer and dialyzed against three changes of one liter of G buffer over 2 d. After a final centrifugation for 1.5 h at 40,000 rpm in a 50.2 Ti rotor at 4°C, the supernatant was aliquoted into Eppendorf tubes, frozen in liquid nitrogen and stored at −80°C. To verify the isolation of actin and its purity, samples from the prepared actin were run on a 10% polyacrylamide gel. Actin concentration was determined using a micro bicinchoninic acid (BCA) protein assay kit (Pierce, Rockford, IL).

The prepared actin was labeled with *N*-hydroxy succinimidyl 5-carboxytetramethyl rhodamine (NHSR; Molecular Probes, Inc., Eugene, OR) following the protocol in Kellog et al. (1988). Slight modifications included the sonication of filamentous actin between cycling procedures to aid disassembly, and a final dialysis step of labeled G-actin against Hepes injection buffer (1 mM Hepes, pH 7.2, 0.2 mM $MgCl_2$, and 0.2 mM ATP). To test for polymerization and visualization of labeled actin, 10 $\mu$M of G-actin was polymerized in F buffer, and then further diluted 1:50 in F buffer. The sample was transferred to a slide, covered with a coverslip and imaged as outlined below.

To prepare phalloidin, a stock solution (0.5 mM) of rhodamine-phalloidin (Molecular Probes, Inc.) in DMSO was diluted with buffer (50 mM K glutamate, 0.5 mM $MgCl_2$, pH 6.5) to a final concentration of 0.1 mM and spun for 5 min in a Beckman microfuge before injection. In some experiments, injected Til neuron cell bodies were also contact-labeled with 3,3'-dioctadecyloxacarbocyanine perchlorate (DiO; Molecular Probes, Inc.) as previously described (O'Connor et al., 1990). In addition, some rhodamine-phalloidin injected cells were bathed in cytochalasin D (Sigma Chemical Co.; 0.01–0.1 $\mu$g/ml) containing culture medium.

### Embryo Culture and Image Analysis

*Schistocerca americana* embryos were obtained from a grasshopper colony at the University of California at Berkeley. Eggs were sterilized, dissected, and staged as previously described (Bentley et al., 1979; Caudy and Bentley, 1986). Limb buds of 31–34% stage embryos were placed on a poly-L-lysine–coated coverslip (5 mg/ml), opened lengthwise, and unrolled flat to expose the pioneer pathway. Mesodermal cells occupying the lumen of the limb were removed with a suction pipette, exposing the Til neurons located on the basal surface of the epithelium. The Til neurons and guidepost neurons were viewed with differential interference contrast optics using a Nikon inverted compound microscope (Lefcort and Bentley, 1987; O'Connor et al., 1990).

A Til neuron cell body was injected with either rhodamine–phalloidin (0.1 mM), rhodamine–actin (0.1 mM) or a mixture of rhodamine–actin and

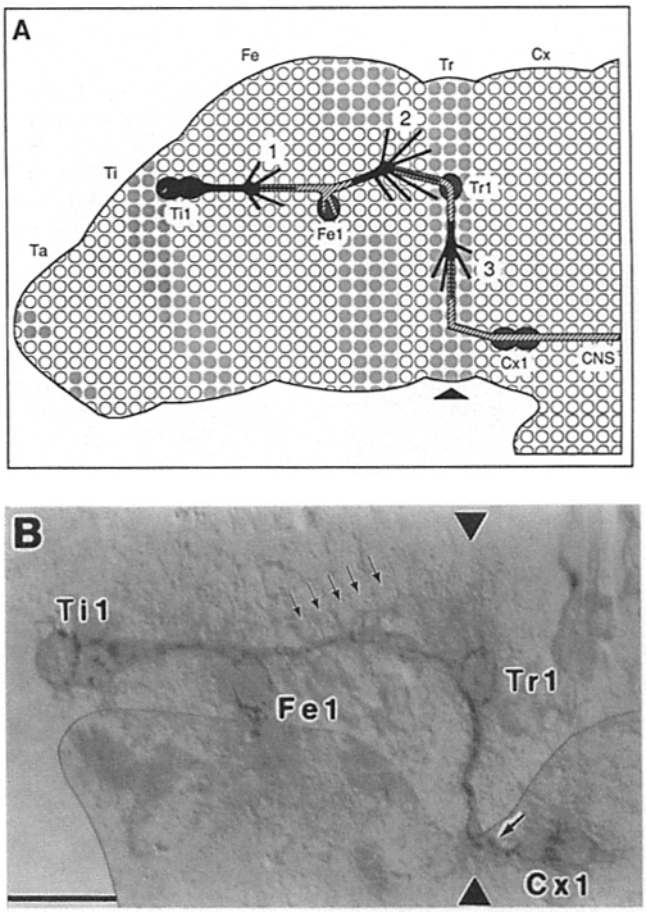


*Figure 1.* The Til pioneer growth cone pathway in the embryonic grasshopper limb bud. (*A*) A schematic representation of the limb at the 33–35% stage of development showing the Til pioneer growth cone pathway, the ectodermal epithelium on which the growth cones migrate and the guidepost cells (Fel, Trl, and Cxl). The sibling pioneer neurons arise in the tibia (Ti) and extend axons along a stereotyped route to the CNS. At three locations, the growth cones make turns mediated by filopodial contact with guidepost cells. Within the trochanter (Tr), the growth cones turn and migrate ventrally along a narrow band of epithelial cells that express fasciclin IV (*filled circles*). The numbers (*1*, *2*, and *3*) beside the filled growth cones indicate the locations of the in situ steering events discussed in the text. *Ta*, tarsus; *Fe*, femur; *Cx*, coxa; *CNS*, border of central nervous system; distal, left; dorsal, up. (*B*) An interference contrast photomicrograph of a limb fillet preparation that has been cultured, fixed and labeled with a neuron-specific antibody (anti-HRP; Jan and Jan, 1982). The Til growth cones have contacted the Fel and Trl guidepost cells, have completed their ventral migration along the fasciclin IV-expressing band of epithelial cells (between *black triangles*), and have made filopodial contact (*large arrow*) with the Cxl guidepost cells. A row of epithelial cells, indicating cell size and spacing, is marked (*small arrows*). Bar, 50 μm.

fluorescein-dextran (0.3 mM, 10 kD; Molecular Probes, Inc.). Injections were made using a pico-spritzer (Narishige USA, Inc., Greenvale, NY) and pulled, beveled borosilicate micropipettes. Before each injection, a slow constant flow of the injection solution from the electrode tip was established. Cell bodies were impaled briefly and the injection solution was allowed to diffuse throughout the cell. Limb preparations were bathed in a modified RPMI medium (Lefcort and Bentley, 1987; O'Connor et al., 1990) at 32–33°C in a heated stage chamber (Medical Instruments, Greenvale, NY) on a Nikon inverted microscope, and imaged with a 1,320 × 1,024 pixel CCD chip (Eastman Kodak Co., Rochester, NY) in a cooled camera (Photometrics Ltd., Tucson, AZ). Images were processed (Perceptics software) on a Mac IIx computer (Apple Computers) and stored on a digital optical disk (Pinnacle). For each group of images, several optical sections were taken through the growth cone. The National Institutes of Health image software also was used for some image analysis and montaging. After image collection, preparations were fixed, and the Til neurons and guidepost cells (pre-axonogenesis neurons) were labeled with neuron-specific antibodies (Jan and Jan, 1982) to confirm their positions (see Fig. 1 *B*).

The results are based on the observation of 36 growth cones in 28 embryos that continued to migrate and steer normally during imaging of injected fluorophores. Of these growth cones, 13 were labeled with rhodamine-phalloidin, 15 with rhodamine-actin, and 8 with both rhodamine-actin and fluorescein-dextran. Growth cones were about equally distributed in the different limb regions.

## Results

To observe actin distribution and dynamics in growth cones in situ, 32–34% stage grasshopper embryo limb bud epithelia were cut open longitudinally along the posterior aspect and unrolled onto an adhesive substrate. With interference contrast optics, the two Til pioneer neurons, the epithelial substrate, and intermediate target cells (guidepost cells) were readily observed in this "fillet" preparation (Fig. 1; O'Connor et al., 1990). On the fillet, growth cones migrated along their normal route, contacting and orienting to normal guidance cues as they proceeded (Lefcort and Bentley, 1987; O'Connor et al., 1990).

### Rhodamine-Phalloidin Injection

Initially, pioneer cell bodies were microinjected with 0.1 mM rhodamine-phalloidin (r-phalloidin). Although the two sibling pioneer cell bodies are coupled by gap-junctions, little rhodamine labeling transferred into the uninjected sibling. After a period of 10–30 min, r-phalloidin diffused to the distal ends of the nascent axons (50–250 μm), and into the growth cones. With the (low) quantities of r-phalloidin that were injected, labeled growth cones continued to migrate at normal rates, ~5–10 μm/h, and responded normally to proximal and circumferential guidance cues, and to guidepost cells. Image stacks of 50–100-ms exposures at 3–6 different focal planes were taken at intervals down to about one every 10 min without disrupting growth cone migration.

r-phalloidin labeling of live growth cones revealed a largely conventional distribution of F-actin (Fig. 2). The nascent axon shaft and the central region of the growth cone contained relatively low levels of F-actin. A bright, thin shell of F-actin occurred in sub-cortical regions, and a core of F-actin occupied the interiors of filopodia. Two aspects of labeling were notable. First, most filopodia in regions of the growth cone perimeter that were extending appeared to contain higher levels of F-actin than other locations around the growth cone perimeter (Fig. 2, *A* and *C*). Second, in some growth cones, bundles of F-actin could be seen extending from the leading edge of the growth cone into central regions and even as far as the shaft of the nascent axon (Fig. 2 *C*).

To confirm that r-phalloidin was selectively labeling F-actin (Forscher and Smith, 1988; Cooper, 1991; Prakash and Pollard, 1991; Ohmori et al., 1992), the culture medium was exchanged for medium containing 0.01–0.1 μg/ml cytochalasin D. Within 1–3 min, the r-phalloidin-labeled material underwent collapse. Collapsing material was retro-

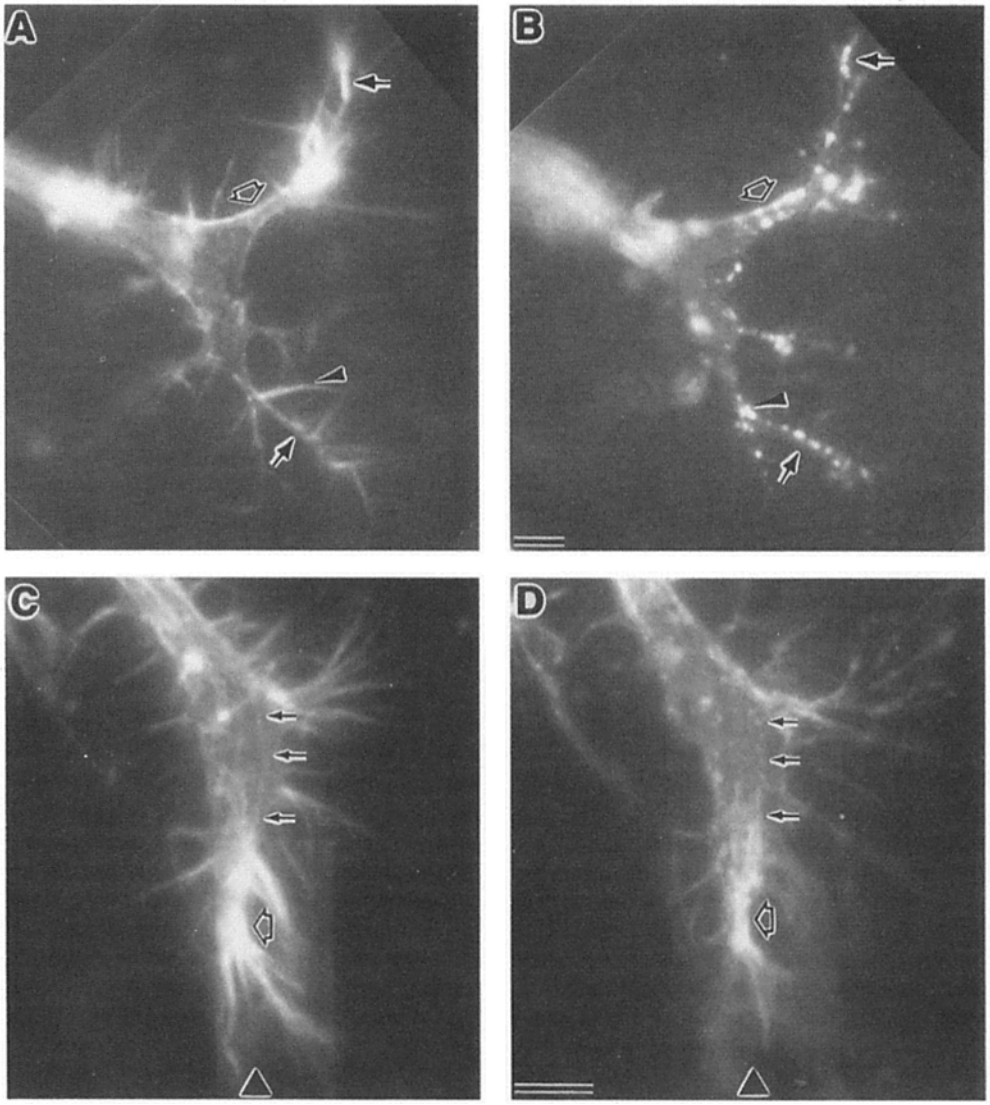


*Figure 2.* Frames from time-lapse image sequences showing rhodamine-phalloidin labeling of F-actin distribution in live Til growth cones migrating in situ on the limb epithelium before (*A* and *C*) and after (*B* and *D*) addition of cytochalasin D to the culture medium. (*A*) A growth cone in the mid-femur (Fig. 1 *A*, location *1*): F-actin is concentrated in the sub-membrane cortex (*open arrow*), in leading branches (*black arrows*) and in filopodia (*arrowhead*). (*B*) The same growth cone 5 min after the addition of cytochalasin D: some filopodia (*arrowhead*) have collapsed back into the growth cone; F-actin in the cortex (*open arrow*) and in small branches (*black arrows*) has collapsed into a series of local accumulations. (*C*) A growth cone migrating ventrally along the fasciclin IV expressing band of epithelial cells (*black triangle*) in the trochanter (Fig. 1 *A*, location *3*): F-actin is concentrated in leading filopodia and the leading edge of the growth cone (*open arrow*). Several F-actin bundles, one of which is labeled by the arrows, extend from the leading edge back through the growth cone into the nascent axon shaft. (*D*) The same growth cone 8 min after the addition of cytochalasin D: the most prominent F-actin bundle (*arrows*) and other bundles have collapsed into a series of labeled aggregates. *C* and *D* are montages of images from two focal planes. Bars, 5 μm.

gradely transported from some filopodia and small branches. Usually, the linear arrays of labeling material, including those that extended through the central region of the growth cone (Fig. 2 *C*), became redistributed into a string of small dots and clumps (Fig. 2, *B* and *D*). In some cases, these dots were retrogradely transported into the growth cone, but in other cases they remained in distal locations. While some filopodia withdrew with the loss of r-phalloidin–labeled material (Fig. 2 *B*), other filopodia remained extended for several tens of minutes. Over a period of hours, they gradually withdrew into the growth cone. Replacement of the cytochalasin medium with normal culture medium resulted in re-extension of filopodia and a resumption of growth cone motility. These results support the conclusion that r-phalloidin is revealing the disposition of F-actin.

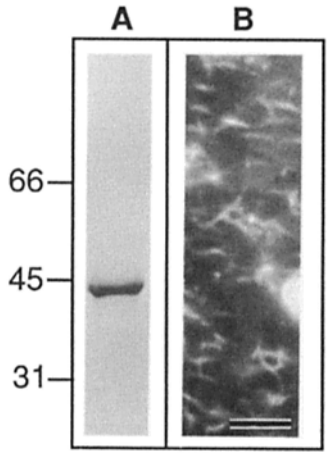


*Figure 3.* Rhodamine-labeled actin. (*A*) A silver stained 10% polyacrylamide gel showing the degree of purity of the actin that was labeled with rhodamine and injected into the Til cells. (*B*) An image of rhodamine-labeled actin filaments polymerized in vitro. Bar, 10 μm.

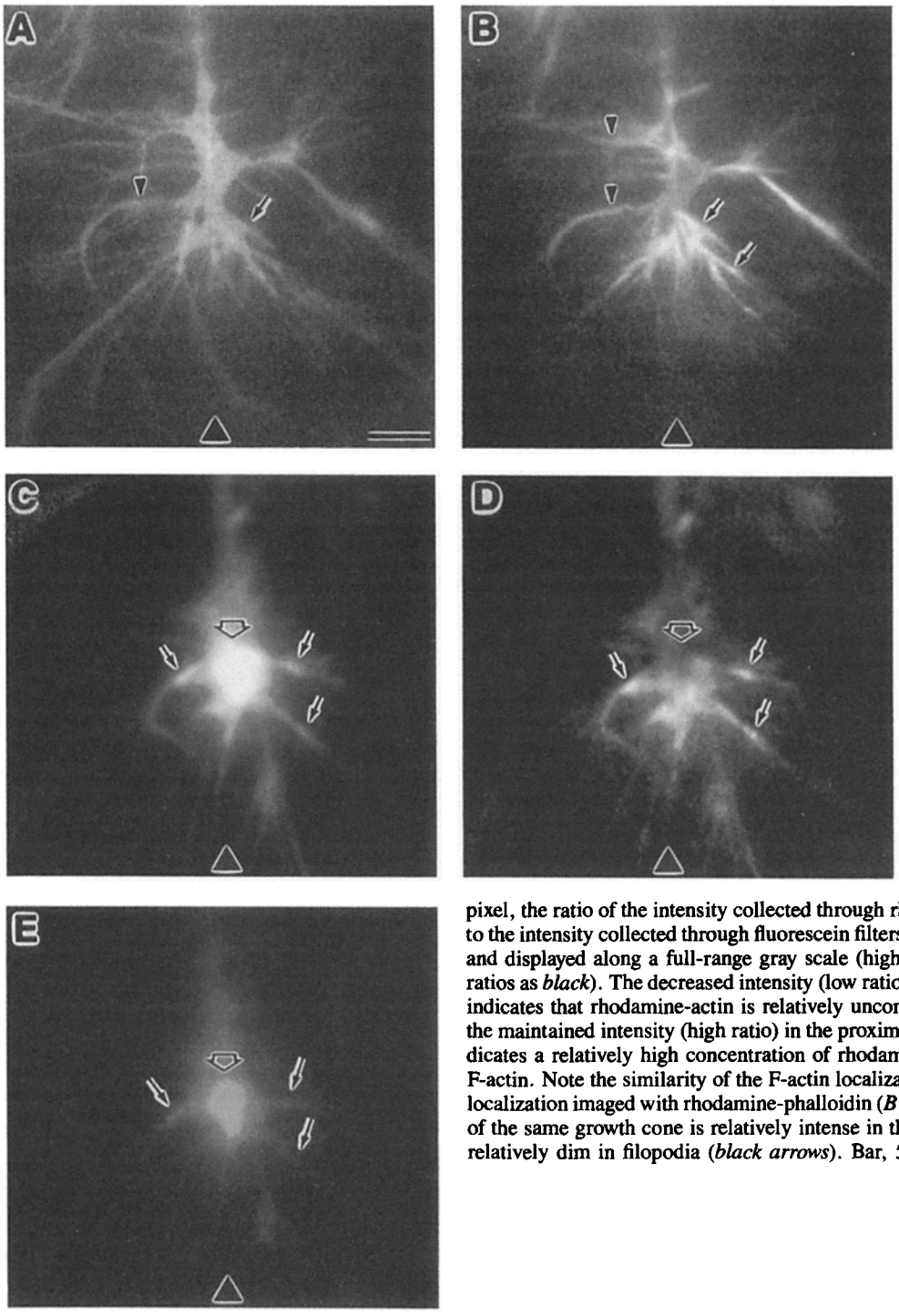


*Figure 4.* Distribution of rhodamine-actin in pioneer growth cones. (*A* and *B*) A live Til growth cone that has been doubled-labeled with DiO and rhodamine-phalloidin, and is migrating ventrally along the fasciclin IV-expressing epithelial band (*black triangle*; all panels) in the trochanter (Fig. 1 *A*, location *3*). (*A*) DiO label: the overall morphology of the growth cone, nascent axon, and filopodia are revealed (the *arrowhead* and *arrow* refer to the corresponding sites in *B*). (*B*) Rhodamine-phalloidin label: F-actin is concentrated in bundles that occupy the cores of leading filopodia and extend into the growth cone. F-actin concentration is much lower in laterally extending filopodia (*arrowheads*). (*C–E*) A different Til growth cone at the same location that has been double-labeled with rhodamine-actin and fluorescein-dextran (10 kD). (*C*) Rhodamine-actin labeling is relatively intense in the central region of the growth cone (*open arrow*) and in leading filopodia (*black arrows*). (*D*) The same growth cone viewed as a ratioed image: for each pixel, the ratio of the intensity collected through rhodamine filters (rhodamine-actin) to the intensity collected through fluorescein filters (fluorescein-dextran) is computed and displayed along a full-range gray scale (high ratios are displayed as *white*, low ratios as *black*). The decreased intensity (low ratio) of the central region (*open arrow*) indicates that rhodamine-actin is relatively unconcentrated in this area; in contrast, the maintained intensity (high ratio) in the proximal regions of filopodia (*arrows*), indicates a relatively high concentration of rhodamine-actin, probably in the form of F-actin. Note the similarity of the F-actin localization revealed by this process to the localization imaged with rhodamine-phalloidin (*B*). (*E*) Fluorescein-dextran labeling of the same growth cone is relatively intense in the central region (*open arrow*), but relatively dim in filopodia (*black arrows*). Bar, 5 μm.

### *Rhodamine-Actin Injection*

Because of the possibility that r-phalloidin interaction with actin polymer might influence actin dynamics, we examined actin dynamics directly with rhodaminated actin (r-actin). Rabbit skeletal muscle actin was labeled with rhodamine and cycled twice through polymerization and depolymerization steps to select for assembly competent labeled actin monomer (Kellogg et al., 1988). The labeled actin product appeared to be quite pure (Fig. 3 *A*), and readily polymerized into filaments under in vitro conditions (Fig. 3 *B*).

In general, growth cones labeled with r-actin (and imaged in several focal planes) appeared similar to those labeled with r-phalloidin (see Figs. 5 *A*, 6 *A*, and 8 *B*). Label was not observed in the uninjected sibling (see Fig. 6 *A*), indicating that little unbound rhodamine was present in the injected material. Labeling intensity was relatively low in the axon shaft (Figs. 4 *C*, 5 *D*, 6 *A*, and see Fig. 8, *A* and *B*), and was

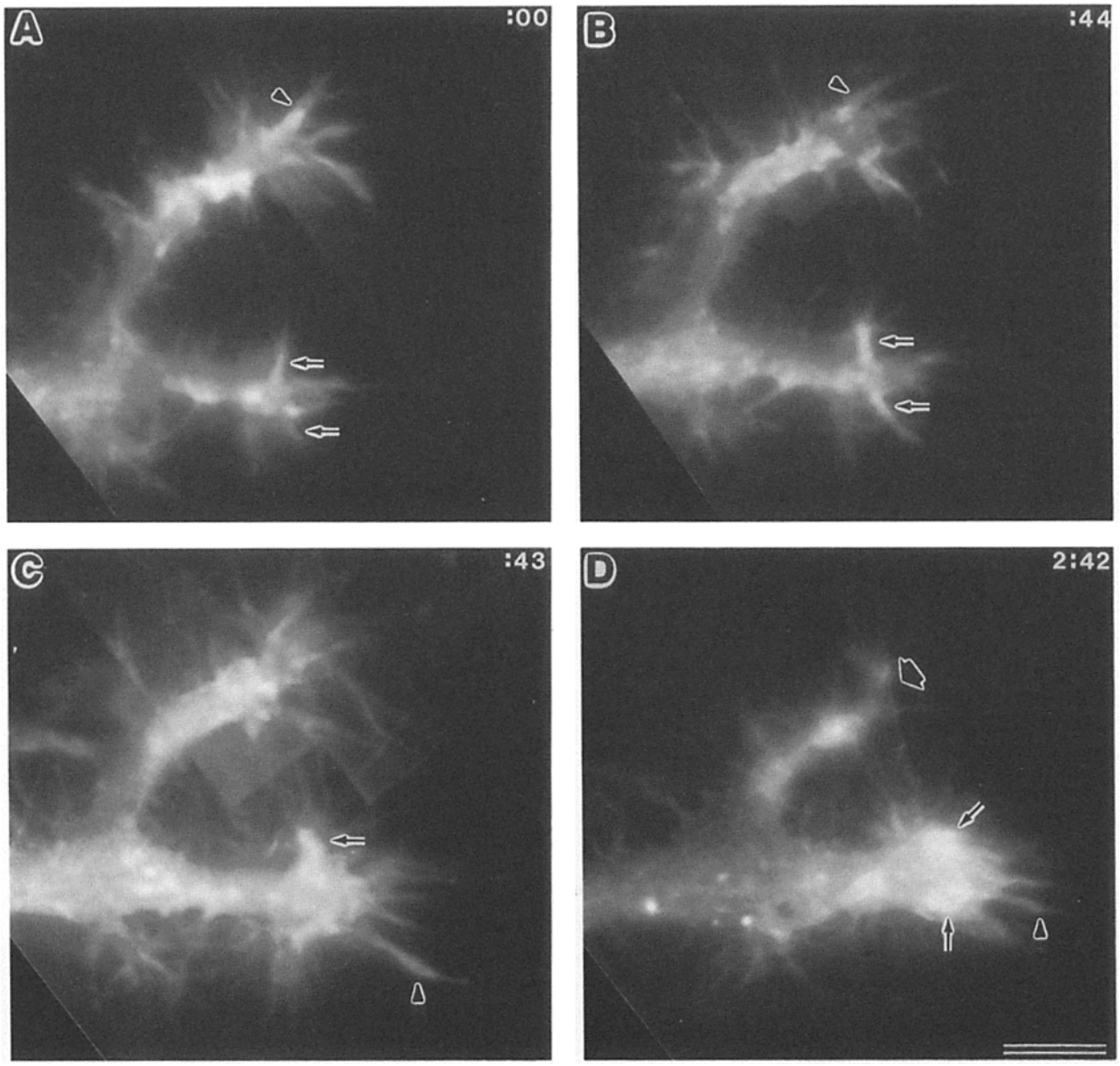


*Figure 5.* Shift in actin distribution during a Til growth cone steering decision in the mid-femur (see text). Frames are from a time-lapse image sequence of a rhodamine-actin labeled Til neuron extending an axon proximally in the mid-femur (Fig. 1 *A*, location *1*). The axon has bifurcated and is extending one growth cone in a dorsal (less preferred) direction, and the other in the proximal (preferred) direction. Initially, the dorsal branch is more robust and grows more rapidly than the ventral branch. However, during the period shown (*A–D*), the dorsal growth cone is withdrawn and the ventral growth cone advances. Actin labeling initially is bright in leading branches of the dorsal growth cone (*A*, *arrowhead*), but subsequently is reduced (*B*, *arrowhead*), and eventually is barely detectable as the branch is withdrawn (*D*, *large arrowhead*). In the ventral growth cone, lightly labeling actin cores initially are seen in processes at the front of the growth cone (*A*, *arrows*); these subsequently become much more robust (*B* and *C*, *arrows*), and one becomes the core of a leading branchlet (*C*, *arrowhead*). Eventually, bright patches of actin occupy the leading edge of the ventral growth cone (*D*, *arrows*), and actin accumulates in the proximal regions of some leading filopodia (*D*, *arrowhead*). Time (h:min, upper right of panels): elapsed time between images in successive panels. Panels are montages of images from two focal planes. Bar, 10 μm.

brightest at the leading edge of the growth cone (Figs. 5 *D*, 6 *A*, and see Fig. 8 *B*). In some images taken through a 60× objective (Fig. 4 *C*), and in many images taken through 100× objectives (Fig. 6, *B–E*), the central region of the growth cone appeared relatively bright. To evaluate whether this labeling was due to F-actin or to a large amount of actin monomer in the larger volume of the central region of the growth cone, pioneer neurons were co-injected with fluorescein–dextran (Fig. 4 *E*) and with r-actin (Fig. 4 *C*). Fluorescein–dextran (10 kD) should distribute relatively uniformly throughout the available intracellular volume (Luby-Phelps et al., 1988), and was used as a monitor of local intracellular

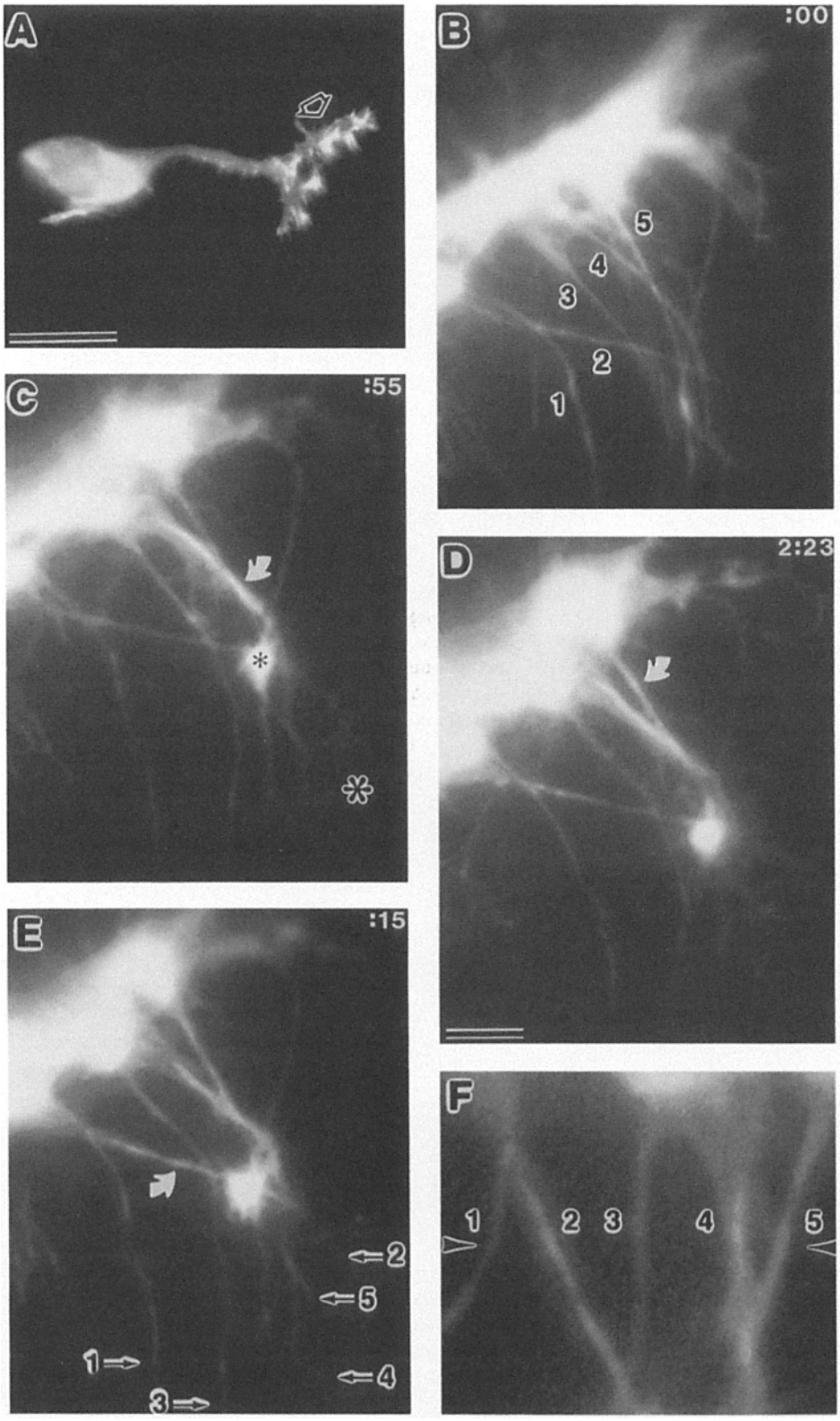


*Figure 6.* Selective actin accumulation in the proximal regions of filopodia that have contacted a guidepost cell (see text). Panels show frames from an image sequence of a live Til growth cone injected with rhodamine–actin and migrating in situ on the limb epithelium. (*A*) The growth cone (*arrow*) is migrating dorsally and proximally in the femur (Fig. 1 *A*, location *2*). (*B*) Several filopodia, with similar actin density, project toward the Trl guidepost cell (*C*, *large asterisk*; the position of Trl was confirmed with interference contrast optics and, after imaging, by labeling the fixed limb with neuron-specific antibodies; see text). Of the five numbered filopodia, 1 and 3 extend ventrally, do not contact cell Trl, and do not accumulate actin. Filopodia 2, 4, and 5 extend ventrally and proximally, contact cell Trl, and accumulate a denser core of actin. The positions of the tips of these five filopodia are shown in *E*. (*C*) Actin has accumulated in the proximal region of filopodium 4 (*curved arrow*); lamellae (between *arrow* and base of filopodium) are extending laterally from the shaft. (*Large asterisk*) position of cell Trl; (*small asterisk*) a lamella or, possibly, filopodial anastomosis. Filopodium number 4 bypasses this lamella. (*D*) Actin has accumulated in the proximal region of filopodium 5 (*curved arrow*). (*E*) Actin has accumulated in the proximal region of filopodium 2 (*curved arrow*). Ventrally extending filopodia 1 and 3 remain unchanged. Numbered arrows, positions of the tips of the five filopodia. (*F*) Detail of (*E*) (rotated ~45° clockwise), indicating the line (between arrowheads) of pixel intensity measurement and the enumeration of filopodia shown in Fig. 7 *A* (and 6 *B*). Time (h:min, on upper right of *B–E*): elapsed time between images in successive panels. Bars: (*A*) 20 μm; (*B–E*) 5 μm (on *D*); (*F*) 2.5 μm (on *D*).

cell volume. Migrating growth cones of eight double-labeled neurons were analyzed. Images were computed which displayed the ratio of r-actin fluorescence to fluorescein–dextran fluorescence in each region of the growth cone (Fig. 4 *D*). In the ratio image, the area of brightness seen in the central region of the growth cone was reduced relative to the brightness of leading filopodia (Fig. 4 *D*, *small arrows*), indicating that actin is more concentrated in leading filopodia. Since no mechanism for local intracellular concentration of actin has been described other than polymerization,

this local increase in actin concentration suggests that the filopodia contain a higher ratio of F-actin to G-actin than the central region of the growth cone. The increased concentration of F-actin indicates that more actin filaments, or longer actin filaments, are present per unit volume. This is likely to be achieved by increasing the packing density of actin filaments through bundling. These areas also correspond well to the pattern of F-actin revealed by r-phalloidin labeling of growth cones in the same location in the limb (Fig. 4 *B*). These results suggest that r-actin accumulation is an indicator of the probable location of F-actin within filopodia.

### *Actin Distribution during Growth Cone Steering in the Distal Femur*

Til pioneer neurons arise at the tibia/femur boundary and their growth cones initially migrate through the distal region of the femur (Fig. 1, location *1*). The growth cones are migrating on the alkaline-phosphatase expressing domain of epithelial cells (Chang, et al., 1993), and may be oriented by a substrate-bound molecular gradient (Norbeck et al., 1992; Wang and Denburg, 1992). Growth cone behavior suggests that the guidance information in this region is relatively ambiguous; numerous course-correcting turns are made, and multiple branches can arise which extend in off-axis directions (O'Connor et al., 1990). Steering in this region primarily occurs by selective retention of processes which have been extended in the axial direction.

We imaged 11 growth cones migrating in the distal femur, six labeled with r-actin and five labeled with r-phalloidin. The distribution of actin in filopodia was similar when viewed with either label. During growth cone migration in this region, redistributions of actin were observed which were correlated with the success of a process in sustaining growth. This was most evident where a growth cone bifurcated and extended two similar sized branches in different directions. Fig. 5 shows a case where a single Til neuron has established two growth cones extending proximally in the femur. At the beginning of the series of images, the dorsal growth cone had extended farther than the ventral growth cone. The extension of the dorsal growth cone was correlated with an increase in the amount of actin at the leading edge and in the leading filopodia. Subsequently, there was a substantial shift in the amount of actin observed in each growth cone (Fig. 5, *B–D*). Actin concentrations, likely to be F-actin bundles, began to build-up in the proximal regions of the majority of filopodia extended from the ventral growth cone (Fig. 5 *A*); these bundles eventually became cores of lamellar processes with a leading fringe of short filopodia (Fig. 5, *B* and *C*). The increase in actin in the ventral growth cone was followed by the extension of the growth cone to and beyond the axial position of the dorsal growth cone (Fig. 5, *C* and *D*). Concomitant with the increase of actin in the ventral growth cone, there was a decrease in the actin concentration in the dorsal growth cone. As the amount of actin deceased in the dorsal growth cone, it started to retract (Fig. 5 *D*). These local changes in actin concentration were detectable before the large-scale withdrawal or substantial advance of the growth cones.

### *Actin Distribution during Turns Toward Guidepost Cells*

At three locations in the limb, pioneer growth cones are reoriented by guidepost cells, and turn to contact them (Fig. 1). The nature of these turns is different from growth cone steering in the distal femur. Although a few filopodia often contact these cells, a single filopodial contact is sufficient to mediate the turn (O'Connor et al., 1990). In the latter situation, the single filopodium dilates at its base to form a small branch, which gradually is converted into the axon.

We observed actin distribution in nine growth cones which were interacting with the Trl (4) or Cxl (5) guidepost cells. Five growth cones were labeled with r-actin, and four with r-phalloidin. The distribution of actin as seen with either label was similar. Four of these growth cones were observed undergoing filopodial dilation as they turned toward the guidepost cells. We observed a selective accumulation of actin in filopodia that were contacting the guidepost cell. A local patch of actin arose in the tips of these filopodia, and a continuous core of actin began to build up in the proximal regions of the filopodia.

Fig. 6 shows an example of these events. A Til growth cone labeled with r-actin has contacted and passed cell Fel, and is extending proximally and dorsally in the proximal femur (Fig. 1, location *2*). Patches of r-actin labeling are arrayed along the leading edge (Fig. 6 *A*). Filopodia, averaging 20–30 $\mu$m in length, are protruded around the growth cone (Fig. 6 *B*). Some of these are directed proximally and ventrally, approximately perpendicular to the shaft of the growth cone, and extend toward the Trl guidepost cell (Fig. 1, *A* and *B*). At the stage shown in Fig. 6 *B*, five lateral filopodia, numbered 1–5, are about equivalent in r-actin intensity. Filopodium number 4, and possibly 5, (Fig. 6 *B*, *numbers*), have established contact with cell Trl. Filopodium number 2 is extending toward cell Trl, and filopodia numbers 1 and 3 are extending distal and ventral to cell Trl (cell Trl is not labeled but is identifiable as follows: in the fillet, the mesodermal cells on the luminal side of the basal lamina have been removed with a suction pipette; the Trl cell, and other neurons, are distinguished from epithelial cells because they have about four times the cross-sectional area of epithelial cells, see Fig. 1 *B*; Trl is the only neuron in the trochanter at this stage of development; therefore, the single, large, adepithelial cell observed with interference contrast optics in the trochanter is Trl; also, the locations of the guidepost cells, including Trl, were confirmed after each experiment by fixation and labeling with neuron-specific antibodies; see also, O'Connor et al., 1990).

In the ensuing period (Fig. 6 *C*), filopodium number 4 has changed. It has accrued a denser core of actin, which extends ~20 $\mu$m distally within the filopodium, starting at its base. In addition, lamellae have spread laterally from about the first 15 $\mu$m of the filopodial shaft. The r-actin intensity in filopodia numbers 1–3 and 5 has not changed substantially. In the next period shown (Fig. 6 *D*), filopodium number 5 (in contact with cell Trl) also has accrued a denser core of r-actin, which extends about 10–15 $\mu$m distally from its base. The r-actin intensity has not changed in filopodia numbers 1–3. During the last period shown (Fig. 6 *E*), filopodium number 2 (in contact with cell Trl) has accrued a core of r-actin label which extends ~15 $\mu$m distally from its base. Filopodia numbers 1 and 3, whose ventrally located tips can be seen in this image, have not contacted cell Trl, and have not accrued a dense core of r-actin.

To quantify these observations we measured peak pixel intensity along the lengths of individual filopodia at successive

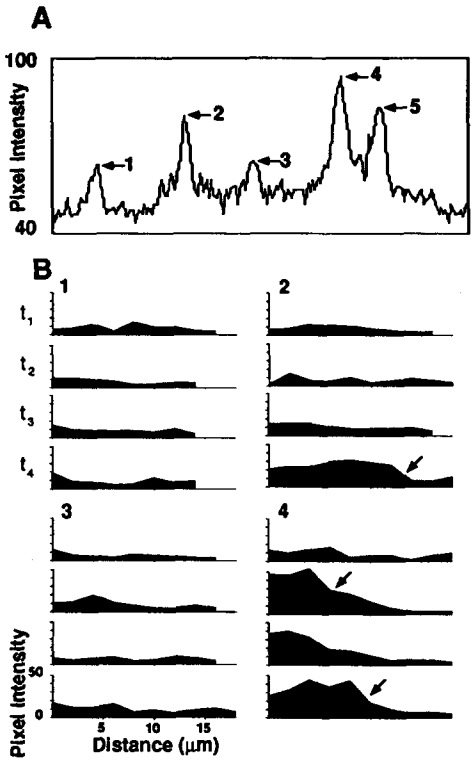


*Figure 7.* Quantification of actin accumulation in filopodia. (*A*) A sample transect showing peak pixel intensities (*arrows*) for the five filopodia shown in Fig. 6 *F*. (*B*) For each filopodium, the peak pixel intensity above background was plotted every 2 μm from the base toward the tip (e.g., *B*, *1*, $t_1$). Background intensities were measured about one filopodial diameter lateral to each transect. This procedure was repeated for images taken at four times: $t_1$, $t_2$ ($t_1$ + 55 min), $t_3$ ($t_2$ + 143 min), $t_4$ ($t_3$ + 15 min). Plots are shown for two filopodia (*1* and *3*) which do not contact cell Tr1, and for two filopodia (*2* and *4*) which do contact Tr1. Filopodia which contact Tr1 accumulate higher concentrations of actin. The actin concentration builds up in the proximal region of the filopodium (*2*, $t_4$; *4*, $t_2$–*4*). Within a filopodium, the discontinuity between the proximal region of higher actin concentration, and the distal region of lower actin concentration can be quite abrupt (*arrows*: *2*, *4*).

times during the growth cone turn to Tr1. First, a transect of pixel intensities was taken across the set of five filopodia which were under observation. The location of the transect is shown in Fig. 6 *F*, and the pixel intensities are shown in Fig. 7 *A*. The transect confirmed that r-actin intensity was higher in filopodia numbers 2, 4, and 5 than in 1 and 3. The brighter filopodia (2, 4, and 5) do not appear to be broader, suggesting that the increased brightness is not due to an increase in diameter (volume). Peak pixel intensities were recorded and plotted against the length of the filopodium at 2-μm intervals from the base toward the tip. In Fig. 7 *B*, r-actin intensity profiles are shown for filopodia 1–4. Finally, these profiles were plotted at four stages during the period in which the r-actin core was developing in filopodia 2 and 4 (Fig. 7 *B*, $t_1$–$t_4$).

At the onset of these measurements, filopodia 1–4 were all 15–20 μm long and had similar, somewhat variable, r-actin intensities. In filopodia 1 and 3, which did not contact cell Tr1, r-actin intensity fluctuated within a low range, and did not build-up during the course of observations. By contrast, in filopodia 2 and 4, which did contact cell Tr1, there was a two to four-fold increase in average r-actin intensity. This increase occurred first in filopodium 4 (between $t_1$ and $t_2$), and later in filopodium 2 (between $t_3$ and $t_4$). In both filopodia, the continuous build-up in actin concentration occurred from the base outwards. The distal end of the r-actin core within filopodia had a quite abrupt distal edge (Fig. 7 *B*, *arrows*). The quantitative measurements of actin distribution confirmed the impressions from the images.

### *Actin Distribution during Turns along an Epithelial Cell Band*

The interior of the trochanter at the 33% stage comprises a circumferential band of epithelial cells, about three cell diameters in width, that express fasciclin IV (Kolodkin et al., 1992). Upon encountering this band, the pioneer growth cones, cease proximal growth, initially extend circumferential branches both dorsally and ventrally, and finally turn and migrate ventrally along the fasciclin IV band toward the Cx1 guidepost cells (Fig. 1, location *3*). During this circumferen-

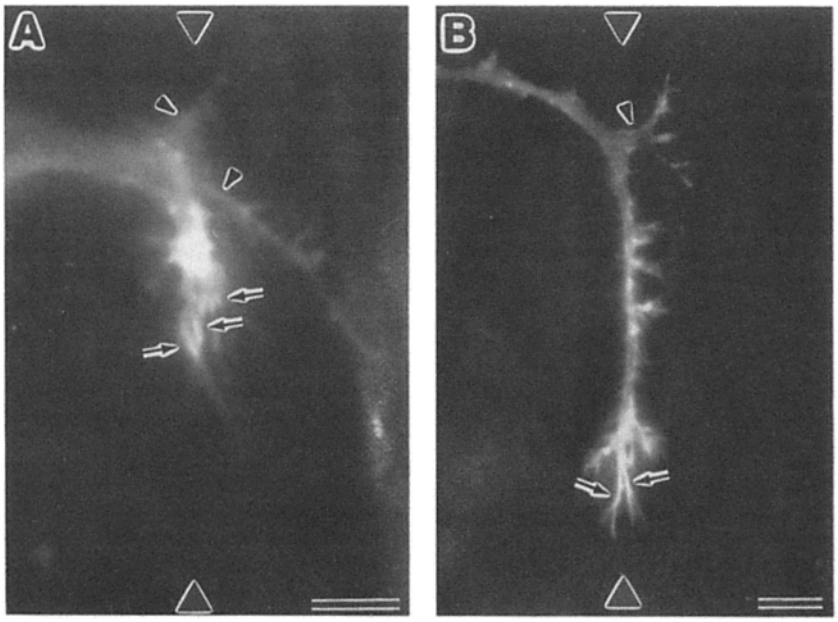


*Figure 8.* Actin distribution in Ti1 growth cones turning and extending ventrally along the fasciclin IV-expressing epithelial band (between *black triangles*) in the trochanter. (*A*) Frame from a time-lapse image sequence of a growth cone, labeled with rhodamine-actin, that is just completing the turn onto the fasciclin IV band (Fig. 1 *A*, location *3*). Most leading filopodia (*arrows*) have denser actin cores in their proximal regions. Dorsally and proximally extending filopodia and branches (*arrowheads*), that are not being followed by the growth cone, do not have denser actin cores. (*B*) A different growth cone just completing the ventral migration also has denser actin cores in the proximal regions of leading filopodia (*arrows*). Actin concentrations are lower along the nascent axon and in lateral branches (*arrowhead*) that are not being followed by the growth cone. Bars, 10 μm.

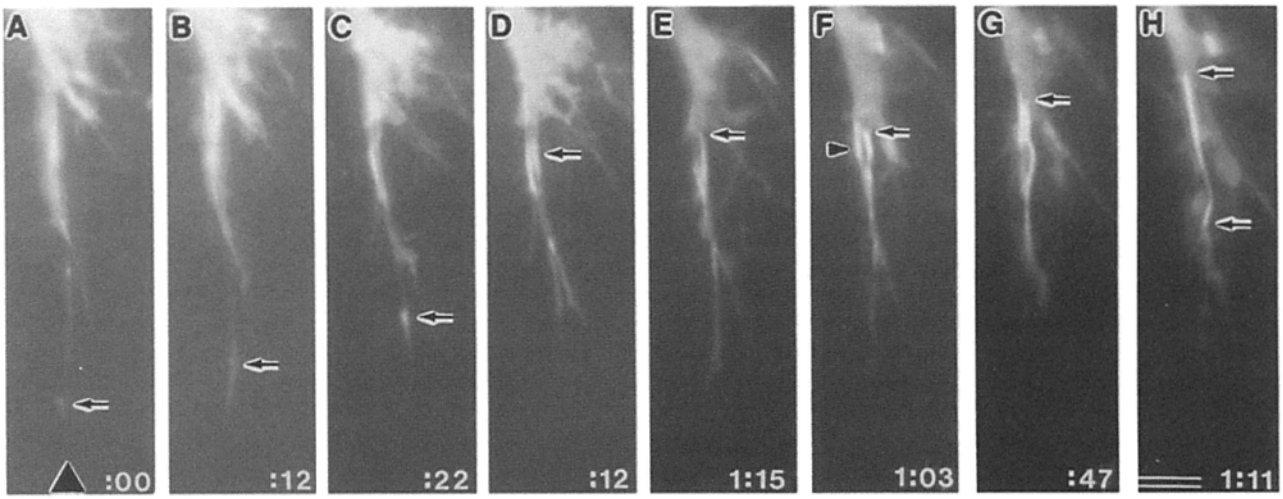


*Figure 9.* Retrograde transport of actin in leading filopodia. (*A–H*) Frames from a time-lapse image sequence of a rhodamine-actin labeled Til growth cone beginning ventral migration along the fasciclin IV-expressing epithelial band in the trochanter (Fig. 1 *A*, location *3*). (*A–C*) Two long, leading filopodia extend ahead of the growth cone. An aggregation of labeled actin (*arrow*) arises at the tip of one filopodium and is retrogradely transported toward the base (*B* and *C*, *arrows*). (*D–H*) A dense core of actin (*arrows*) with an abrupt proximal boundary (*F* and *H*, *arrows*) accumulates in the proximal region of the filopodium. This core, which is likely to be a bundle of F-actin, eventually becomes ~13 μm long (*H*, between *arrows*), has a quite sharp distal boundary (*H*, *lower arrow*), and is slowly retrogradely transported into the central region of the growth cone (*F–H*, *arrows*). A similar dense core of actin (*F*, *arrowhead*) also accumulates in the proximal region of the other leading filopodium. Time (h:min, lower right of panels): elapsed time between images in successive panels. Bar, 5 μm.

tial migration, we monitored actin distribution in eight growth cones, four injected with r-actin, and four injected with r-phalloidin. Actin distribution appeared to be similar in both classes of growth cones.

As observed in growth cones in other regions of the limb, actin labeling was higher in most leading filopodia, and lower in filopodia and branches extended in other directions (Fig. 8). Both in growth cones that were commencing ventral growth (Figs. 8 *A* and 9 *F*), and in those that were completing the ventral migration (Fig. 8 *B*), cores of labeling actin were observed in the proximal regions of filopodia extending ventrally along the fasciclin IV band.

Several possible mechanisms could result in the accumulation of actin in the proximal regions of leading filopodia. One of these is an increase in the retrograde transport of actin. As noted earlier, retrograde transport of r-phalloidin labeled F-actin was seen in filopodia after application of cytochalasin D (Fig. 2). Retrograde transport of small clumps of r-actin along filopodia also was observed. An example of this phenomenon is illustrated in Fig. 9. Here, an r-actin labeled growth cone has turned ventrally along the fasciclin IV expressing band of epithelium. Two leading filopodia, ~25 μm in length, extend ventrally along the band. In one of these, a large aggregation of actin labeling appears at the tip and is retrogradely transported, at a rate of 0.25–1.0 μm/min, to the base (Fig. 9, *A–C*). At the base, it accumulates into a continuous core of actin, which eventually reaches a length of ~13 μm (Fig. 9, *D–G*). This solid core of actin is retrogradely transported into the central region of the growth cone (Fig. 9, *F–H*), until it extends at least 6 μm centrally from the base of the filopodium. The rate of retrograde transport of this actin core is slower than the rate of transport distally in filopodia. A similar core of actin is seen in the other leading filopodium (Fig. 9 *F*), and it also is retrogradely transported into the central region of the growth cone. Similar structures are seen in another growth cone at the same location labeled with r-phalloidin (Fig. 2 *C*), and these structures are disassembled by cytochalasin (Fig. 2 *D*). These structures appear likely to be F-actin bundles.

## Discussion

### Actin Distribution in Neuronal Growth Cones In Situ

We report here the first observations of actin distribution and dynamics in neuronal growth cones migrating in situ. Actin distribution was imaged in live growth cones with intracellularly injected rhodaminated-phalloidin and with rhodaminated rabbit muscle actin. r-phalloidin labels F-actin with relatively high affinity; labeled structures were confirmed as F-actin by rapid disassembly in the presence of cytochalasin D (Fig. 2; Forscher and Smith, 1988; Cooper, 1991; Prakesh and Pollard, 1991; Ohmori et al., 1992). r-actin occurs both as monomer and polymer. In most preparations, r-actin labeling (Figs. 5 *A*, 6 *A*, and Fig. 8, *A* and *B*) was similar to r-phalloidin labeling (Figs. 2 and 4 *B*), with light labeling in the axon and relatively intense labeling in the growth cone. This suggests that much of the labeling seen with r-actin probably was F-actin, which should be concentrated in the growth cone, rather than monomeric actin, which should be relatively uniformly distributed throughout the cell. Within r-actin–labeled growth cones, the central growth cone domain sometimes appeared as bright as the filopodia (Figs. 4 *C*, 5 *D*, and 6 *B*). Ratio imaging with fluorescein-dextran (Fig. 4 *E*) and r-actin (Fig. 4 *C*) demonstrated that labeling in the central region is not due to high actin concentration, but rather to the increased volume of the growth cone in this region (Fig. 4 *D*). Ratio imaging also confirmed the presence of concentrated actin, likely to be F-actin, within filopodia.

Thus, r-actin labeling appears to be an indicator of the probable distribution of F-actin within filopodia.

The distribution of F-actin in Til growth cones migrating in situ generally was similar to that described in growth cones in vitro (Letourneau, 1983; Bridgman and Dailey, 1989; Lewis and Bridgman, 1992). As observed with r-phalloidin and r-actin, a shell of cortical F-actin surrounded the nascent axon and growth cone. The interior of the axon and the base of the growth cone were relatively devoid of F-actin. Bright labeling occurred in the growth cone perimeter and the proximal regions of filopodia. In some cases, actin cores extending proximally from filopodia appeared to terminate in peripheral lamellae extending from the growth cone (Fig. 6, *E* and *F*, filopodium *4*), or near the central domain of the growth cone (Fig. 4, *B* and *D*, and Figs. 8 and 9 *H*). But in other cells, multiple F-actin bundles appeared to traverse the central region of the growth cone (Fig. 2 *C*), and continue into the nascent axon. In neurons examined in vitro, considerable variation in F-actin bundle termination sites within growth cones also has been observed. In *Aplysia* bag cell growth cones in vitro, the distribution of microtubules and of F-actin bundles is virtually complementary, with peripheral F-actin bundles ending at the interface between the central and peripheral domains (Forscher and Smith, 1988). In rat SCG neurons, F-actin bundles often ended near the bases of filopodia, or at the intersection with the central domain, but other bundles could extend deep into the growth cone (Lewis and Bridgman, 1992).

### *Growth Cone Steering and Actin Distribution*

We observed actin distribution during growth cone steering in several regions of the limb. In distal regions, growth cones steer along the longitudinal axis of the limb by sustaining and expanding branches extended along the limb axis in preference to branches extended in more off-axis directions (O'Connor et al., 1990). Where growth cones encounter guidepost cells, they extend toward them by expanding filopodia which have contacted the cell surface. When growth cones reach the trochanter, they abruptly cease proximal growth and extend branches in both directions along the limb circumference. Subsequently, the ventrally directed branches are selected for further growth. We observe that in each of these regions, selective growth is accompanied by the accumulation of actin in most of the leading filopodia. This occurs in processes extending along the limb axis (Fig. 5), in processes contacting guidepost cells (Fig. 6), and in processes extending ventrally within the trochanter (Figs. 2 *C*, 4, 8, and 9). On a relatively large spatial scale, where a bifurcated axon transiently establishes multiple growth cones, actin can be seen to erode in branches that are not maintained, and to accumulate in branches that are sustained (Fig. 5). On a finer scale, adjacent filopodia protruding from the margin of a growth cone can have cores containing very different amounts of actin: most of those whose tips contact high affinity guidance cues have higher levels of actin, whereas neighboring filopodia whose tips extend in other directions do not (Figs. 6 and 7). Thus actin accumulation in a particular region of the growth cone perimeter accompanies growth cone turning in that direction. This relationship is similar to that reported for *Aplysia* bag cell growth cones that have contacted other bag cells in vitro (Lin and Forscher, 1993). A complementary situation may occur where growth cones are stalling, collapsing, or retracting. In branches of bifurcated Til axons, substantial erosion of actin from growth cones accompanies branch withdrawal (Fig. 5). Actin concentration is similarly depleted in chick DRG growth cones that have been exposed to a growth cone collapsing factor (Fan et al., 1993). These results suggest that regulation of actin may be a significant element in both positive (attractive) and negative (repulsive) growth cone steering events.

Actin does not accumulate uniformly within leading filopodia. Actin cores with relatively sharp distal and proximal boundaries can build-up in the proximal regions of filopodia (Figs. 4 and 6–9). These cores, which appear likely to be F-actin bundles, secondarily can extend both distally (Fig. 7 *B*) and proximally (Fig. 9, *F–H*). This accumulation of actin corresponds to changes observed with video-imaging of growth cones labeled with lipophilic dyes (O'Connor et al., 1990): when a dye-labeled filopodium contacts the surface of a guidepost cell, the tip expands into a palmate configuration, most of the distal shaft of the filopodium retains its initial diameter, and the proximal region of the filopodium progressively enlarges in a proximal to distal progression. This proximal enlargement is at the location of the actin core, suggesting that the dilation of the filopodium may be caused by the accumulation of F-actin.

Within the growth cone, proximal ends of actin filament bundles may interact with and influence the distribution of microtubules. In fixed material, microtubules regularly are aligned with actin filament bundles (Letourneau, 1983; Gordon-Weeks, 1991; Lewis and Bridgman, 1992), and molecules have been identified that appear to interact both with microtubules and actin filaments (Goslin et al., 1989). Tension generated within actin filament arrays may influence the position and polymerization of microtubules (Heideman et al., 1990; Lamoureux et al., 1992). Recent video observations have demonstrated a rapid translocation of microtubules to sites of F-actin accumulation in *Aplysia* growth cones in vitro (Lin and Forscher, 1993). Video-imaging of migrating Til growth cones labeled with rhodaminated bovine brain tubulin revealed that microtubules selectively entered the bases of dilated filopodia that are in contact with guidepost cells (Sabry et al., 1991). This region is the location of actin accumulation. Therefore, in these growth cones, the initiation of microtubule intrusion into branchlets forming from filopodia appears to be associated with regions of actin concentration.

Several aspects of actin dynamics, including number of nucleation sites, polymerization rate, transport rate, stability, local contraction, and disassembly rate, could contribute to the accumulation of actin in the proximal regions of leading filopodia (Southwick et al., 1989; Maciver et al., 1991; Bearer, 1992; Theriot et al., 1992; Zigmond et al., 1992). While our results do not distinguish among these possibilities, we do observe that aggregations of actin can be retrogradely transported along filopodia in which actin is accumulating (Fig. 9). That filopodia in which accumulation is occurring can extend from the same location at the margin of the growth cone as filopodia in which actin is not accumulating (Fig. 6) supports the idea that accumulation ultimately is due to events occurring at the filopodial tip (Fig. 10).

Distally, actin filament bundles are contiguous with specializations at the tips of filopodia and the leading edges of lamellipodia (Lewis and Bridgman, 1992). At these loca-

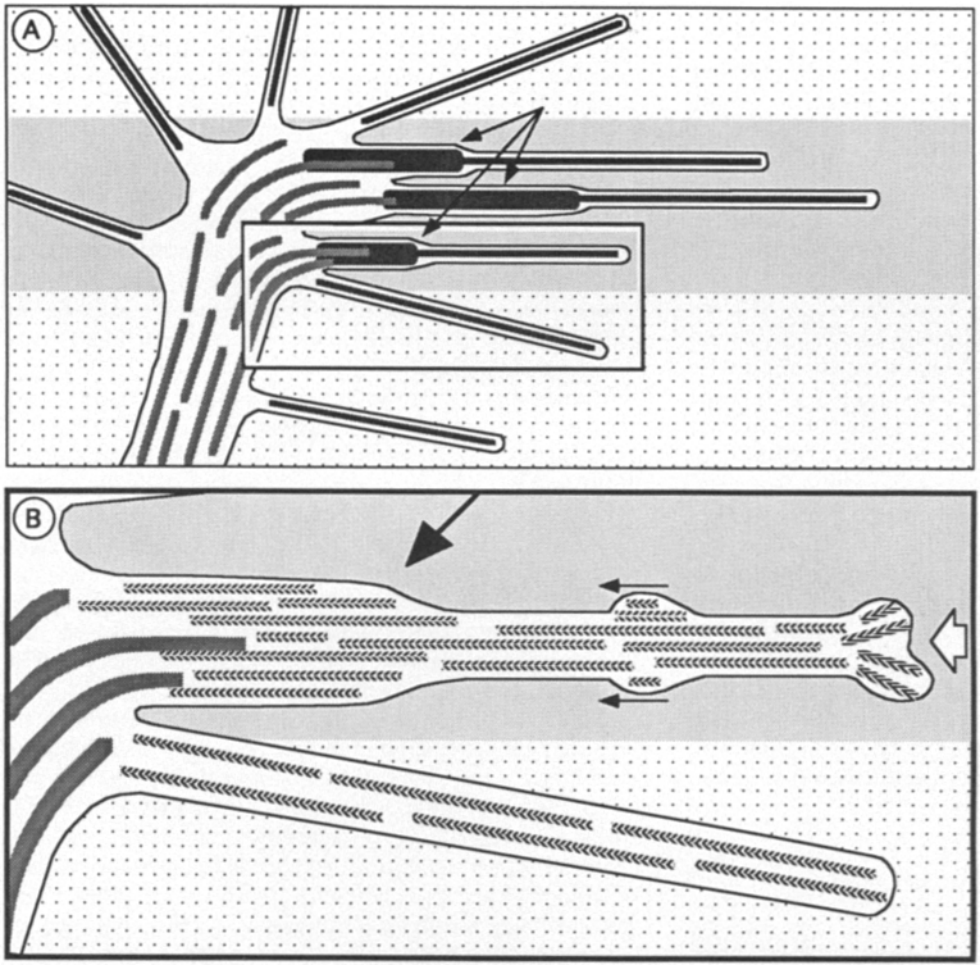


*Figure 10.* Schematic diagrams of steering by pioneer growth cones responding to in situ guidance cues. (*A*) A growth cone that is turning and orienting along a preferred guidance substrate (*darker background*), such as the fasciclin IV expressing epithelial band. Proximal regions of guiding filopodia expand (O'Connor et al., 1990), and microtubules (*light stipple*) selectively invade the proximal regions of expanding filopodia (Sabry et al., 1991). These expanded proximal regions are the sites of dense cores of actin (*arrows*; *dark stipple*), likely to be F-actin, which are not present in other filopodia that are not being followed by the growth cone. (*B*) Detail from *A* (*inset*) showing a possible model of intracellular events: interactions (*open arrowhead*) at the tip of the filopodium between receptors and ligands that mediate guidance may be "encoded" through transmembrane signaling into the generation of more, or more stable, F-actin (*herringbone*). The F-actin may be retrogradely transported, sometimes in large aggregations (*small arrows*) to the proximal region of the filopodium. In the proximal region, dense cores (*large arrow*) of F-actin accumulate (by retrograde transport and perhaps other mechanisms, see text), where they may distinguish filopodia that are interacting with preferred guidance substrates. By a variety of possible mechanisms (see text) these dense cores may selectively accrue microtubules (*stipple*), and thereby influence the direction of consolidation of the forming axon.

tions, interactions with extracellular molecules that effect actin filament nucleation, polymerization, and stability are likely to occur (Southwick et al., 1989; Luna, 1991; Stossel, 1993; Wang et al., 1993). Contact with extracellular features, such as polycationic beads, can initiate local generation of dense bundles of actin filaments (Forscher et al., 1992). Adhesion to a variety of substrates can effect F-actin polymerization and organization (Southwick et al., 1989; Abosch and Lagenaur, 1993). Local alteration of calcium ion concentration can initiate protrusion of filopodia (Davenport and Kater, 1992; Rehder and Kater, 1992; Davenport et al., 1993), presumably a consequence of a local change in actin dynamics (Lankford and Letourneau, 1991). Transmembrane molecules that promote outgrowth, such as L1, N-CAM, and N-cadherin, effect intracellular calcium ion concentration and other second messenger systems (Bixby, 1989; Schuch et al., 1989; Williams et al., 1993). Through such interactions, reception of extracellular guidance information by receptors on filopodia and lamellipodia may regulate actin dynamics.

The build-up of actin in the proximal regions of guiding filopodia prompts speculation about its function. An issue in steering of Til growth cones, and other growth cones with long filopodia (Myers and Bastiani, 1993), is how guidance information detected at the tips of filopodia is effectively conveyed to the base. An interesting possibility is that the amount or stabilization-state of F-actin retrogradely transported to the base of the filopodium could be an element of this message. Transmembrane receptors and associated second messenger systems at the tip could be viewed as "encoding" information about the extracellular environment into more, or more stable, F-actin which could then engage the retrograde transport system at the filopodium tip for translocation to the base (Fig. 10). Accumulation of more, or more stable, F-actin at the base of a filopodium could distinguish its base from the bases of other filopodia contacting less preferred substrates. The presence of this F-actin could be "decoded" by mechanisms, including generation of tension (Heideman et al., 1990; Lamoreux et al., 1992), cross-linking to microtubules (Goslin et al., 1989), or contraction of the local actin meshwork (Yamura and Kitanishi-Yumura, 1992), that selectively accrue microtubules, thereby determining where the nascent axon will be consolidated within the growth cone perimeter.

The specific molecular interactions that mediate pioneer growth cone steering in each limb region are largely undeter-

mined. However, each region does express a quite different set of substrate molecules (see introduction). The hierarchical choices made by the Til growth cones, as well as the demonstrated differences in substrate adhesion and molecular expression, suggest that the growth cones are being guided by different molecular interactions in the different limb regions. The observation that growth cone interactions with each of these substrates results in selective accumulation of actin is consistent with the notion that regulation of actin may be a common signaling path that is downstream from a variety of cell surface molecular interactions mediating guidance.

We thank David Drubin and Michael Ignatius for criticizing a version of the manuscript.

This work was supported by National Institutes of Health grant NS09074-22 and National Science Foundation grant IBN 91-20904.

Received for publication 9 July 1993 and in revised form 31 August 1993.

### *References*

Abosch, A., and C. Lagenaur. 1993. Sensitivity of neurite outgrowth to microfilament disruption varies with adhesion molecule substrate. *J. Neurobiol.* 24:344–355.

Anderson, H., and R. P. Tucker. 1988. Pioneer neurons use basal lamina as a substratum for outgrowth in the embryonic grasshopper limb. *Development (Camb.).* 104:601–608.

Bastiani, M. J., A. L. Harrelson, P. M. Snow, and C. S. Goodman. 1987. Expression of fasciclin I and II glycoproteins on subsets of axon pathways during neural development in the grasshopper. *Cell.* 48:745–755.

Bastiani, M. J., H. G. de Couet, J. M. A. Quinn, R. O. Karlstrom, K. Kotrla, C. S. Goodman, and E. E. Ball. 1992. Position-specific expression of the annulin protein during grasshopper embryogenesis. *Dev. Biol.* 154:129–142.

Bate, C. M. 1976. Pioneer neurons in an insect embryo. *Nature (Lond.).* 260:54–56.

Bearer, E. L. 1992. An actin-associated protein present in the microtubule organizing center and the growth cones of PC-12 cells. *J. Neurosci.* 12:750–761.

Bentley, D., and T. P. O'Connor. 1992. Guidance and steering of peripheral pioneer growth cones in grasshopper embryos. *In* The Nerve Growth Cone. P. C. Letourneau, S. B. Kater, and E. R. Macagno, editors. Raven Press Ltd., New York. 265–282.

Bentley, D., and A. Toroian-Raymond. 1986. Disoriented pathfinding by pioneer neurone growth cones deprived of filopodia by cytochalasin treatment. *Nature (Lond.).* 323:712–715.

Bentley, D., H. Keshishian, M. Shankland, and A. Toroian-Raymond. 1979. Quantitative staging of embryonic development of the grasshopper, *Schistocerca nitens*. *J. Embryol. Exp. Morphol.* 54:47–74.

Bixby, J. L. 1989. Protein kinase C is involved in laminin stimulation of neurite outgrowth. *Neuron.* 2:287–297.

Bridgman, P. C., and M. E. Dailey 1989. The organization of myosin and actin in rapid frozen nerve growth cones. *J. Cell Biol.* 108:95–109.

Caudy, M., and D. Bentley. 1986. Pioneer growth cone steering along a series of neuronal and non-neuronal cues of different affinities. *J. Neurosci.* 6:1781–1795.

Chang, W. S., K. Serikawa, K. Allen, and D. Bentley. 1992. Disruption of pioneer growth cone guidance in vivo by removal of glycosyl-phosphatidyl-inositol-anchored cell surface proteins. *Development (Camb.).* 114:507–519.

Chang, W. S., K. R. Zachow, and D. Bentley. 1993. Expression of epithelial alkaline phosphatase in segmentally iterated bands during grasshopper limb morphogenesis. *Development (Camb.).* 118:651–663.

Condic M. L., and D. Bentley. 1989*a*. Pioneer neuron pathfinding from normal and ectopic locations in vivo after removal of the basal lamina. *Neuron.* 3:427–439.

Condic, M. L., and D. Bentley. 1989*b*. Pioneer growth cone adhesion in vivo to boundary cell and neurons after enzymatic removal of basal lamina in grasshopper embryos. *J. Neurosci.* 9:2687–2696.

Cooper, J. A. 1991. The role of actin polymerization in cell motility. *Annu. Rev. Physiol.* 53:585–605.

Davenport, R. W., and S. B. Kater. 1992. Local increases in intracellular calcium elicit local filopodial responses in *Helisoma* neuronal growth cones. *Neuron.* 9:405–416.

Davenport, R. W., P. Dou, V. Rehder, and S. B. Kater. 1993. A sensory role for neuronal growth cone filopodia. *Nature (Lond.).* 361:721–724.

Elkins, T., M. Hortsch, A. J. Bieber, P. M. Snow, and C. S. Goodman. 1990. *Drosophila* fasciclin I is a novel homophilic adhesion molecule that along with fasciclin III can mediate cell sorting. *J. Cell Biol.* 110:1825–1832.

Fan, J., S. G. Mansfield, R. Redmond, P. R. Gordon-Weeks, and J. A. Raper. 1993. The organization of F-actin and microtubules in growth cones exposed to a brain-derived collapsing factor. *J. Cell Biol.* 121:867–878.

Forscher, P., and S. J. Smith 1988. Actions of cytochalasins on the organization of actin filaments and microtubules in a neuronal growth cone. *J. Cell Biol.* 107:1505–1516.

Forscher, P., C.-H. Lin, and C. Thompson. 1992. Novel form of growth cone motility involving site-directed actin filament assembly. *Nature (Lond.).* 357:515–518.

Gordon-Weeks, P. R. 1987. The cytoskeletons of isolated neuronal growth cones. *Neuroscience.* 21:977–989.

Gordon-Weeks, P. R. 1991. Evidence for microtubule capture by filopodial actin filaments in growth cones. *NeuroReport.* 2:573–576.

Goslin, K., E. Birgbauer, G. Banker, and F. Solomon 1989. The role of cytoskeleton in organizing growth cones: a microfilament-associated growth cone component depends upon microtubules for its localization. *J. Cell Biol.* 109:1621–1631.

Heideman, S. R., P. Lamoureux, and R. E. Buxbaum. 1990. Growth cone behavior and production of traction force. *J. Cell Biol.* 111:1949–1957.

Jan, L. Y., and Y. N. Jan. 1982. Antibodies to horseradish peroxidase as specific neural markers in *Drosophila* and grasshopper embryos. *Proc. Natl. Acad. Sci. USA.* 79:2700–2704.

Jay, D. J., and H. Keshishian. 1990. Laser inactivation of fasciclin I disrupts axon adhesion of grasshopper pioneer neurons. *Nature (Lond.).* 348:548–551.

Karlstrom, R. O., L. P. Wilder, and M. J. Bastiani. 1993. Lachesin: an immunoglobin superfamily protein whose expression correlates with neurogenesis in grasshopper embryos. *Development (Camb.).* 118:509–552.

Kellogg, D. R., T. J. Mitchison, and B. Alberts. 1988. Behavior of microtubules and actin filaments in living *Drosophila* embryos. *Development (Camb.).* 103:675–686.

Kolodkin, A. L., D. J. Matthes, T. P. O'Connor, N. H. Patel, A. Admon, D. Bentley, and C. S. Goodman. 1992. Fasciclin IV: sequence, expression and function during growth cone guidance in the grasshopper embryo. *Neuron.* 9:831–845.

Lamoureux, P., J. Zheng, R. Buxbaum, and S. R. Heidemann. 1992. A cytomechanical investigation of neurite growth on different culture surfaces. *J. Cell Biol.* 118:655–661.

Lankford, K. L., and P. C. Letourneau. 1991. Roles of actin filaments and three second-messenger systems in short-term regulation of chick dorsal root ganglion neurite outgrowth. *Cell Motil. Cytoskeleton.* 20:7–29.

Lefcort, F., and D. Bentley. 1987. Pathfinding by pioneer neurons in isolated, opened and mesoderm-free limb buds of embryonic grasshopper. *Dev. Biol.* 119:446–480.

Letourneau, P. C. 1983. Differences in the organization of actin in the growth cones compared with the neurites of cultured neurons from chick embryos. *J. Cell Biol.* 97:963–973.

Lewis, A. K., and P. C. Bridgman. 1992. Nerve growth cone lamellipodia contain two populations of actin filaments that differ in organization and polarity. *J. Cell Biol.* 119:1219–1243.

Lin, C.-H., and P. Forscher, P. 1993. Cytoskeletal remodeling during growth cone target-interactions. *J. Cell Biol.* 121:1369–1384.

Luby-Phelps, K., F. Lanni, and D. L. Taylor. 1988. The submicroscopic properties of cytoplasm as a determinant of cellular function. *Annu. Rev. Biophys. Biophys. Chem.* 17:369–396.

Luna, E. J. 1991. Molecular links between the cytoskeleton and membranes. *Curr. Opin. Cell Biol.* 3:120–126.

Maciver, S. K., D. H. Wachsstock, W. H. Schwarz, and T. D. Pollard. 1991. The actin filament severing protein actophorin promotes the formation of rigid bundles of actin filaments cross-linked with $\alpha$-actinin. *J. Cell Biol.* 115:1621–1628.

Mason, C. A., and P. Godement. 1992. Growth cone form reflects interactions in visual pathways and cerebellar targets. *In* The Nerve Growth Cone. P. C. Letourneau, S. B. Kater, and E. R. Macagno editors. Raven Press Ltd., New York. 402–423.

Mitchison, T., and M. Kirschner. 1988. Cytoskeletal dynamics and nerve growth. *Neuron.* 1:761–772.

Myers, P. Z., and M. J. Bastiani. 1993. Growth cone dynamics during the migration of an identified commissural growth cone. *J. Neurosci.* 13:127–143.

Norbeck, B. A., and J. L. Denburg. 1991. A molecular marker for epithelial morphogenesis in the cockroach. *Roux's Arch. Dev. Biol.* 198:395–401.

Norbeck, B. A., Y. Feng, and J. L. Denburg. 1992. Molecular gradients along the proximo-distal axis of embryonic insect legs: possible guidance cues of pioneer axon growth. *Development (Camb.).* 116:467–479.

O'Connor T. P., J. S. Duerr, and D. Bentley. 1990. Pioneer growth cone steering decisions mediated by single filopodial contacts in situ. *J. Neurosci.* 10:3935–3946.

Ohmori, H., S. Toyama, and S. Toyama. 1992. Direct proof that the primary site of action of cytochalasin on cell motility processes is actin. *J. Cell Biol.* 116:933–941.

Okabe, S., and N. Hirokawa. 1989. Incorporation and turnover of biotin-labeled actin microinjected into fibroblastic cells: and immunoelectron microscopic study. *J. Cell Biol.* 109:1581–1595.

Okabe, S., and N. Hirokawa. 1991. Actin dynamics in growth cones. *J. Neurosci.* 11:1918-1929.
Pardee, J. D., and J. A. Spudich. 1982. Purification of muscle actin. *Methods Enzymol.* 85:164–181.
Pollard, T. D. 1990. Actin. *Curr. Opin. Cell Biol.* 2:33–40.
Prakash, S., and T. D. Pollard. 1991. Effects of cytochalasin, phalloidin and pH on the elongation of actin filaments. *Biochemistry.* 30:1973–1980.
Rehder, V., and S. B. Kater. 1992. Regulation of neuronal growth cone filopodia by intracellular calcium. *J. Neurosci.* 12:3175–3186.
Sabry, J. H., T. P. O'Connor, L. E. Evans, A. Toroian-Raymond, M. Kirschner, and D. Bentley 1991. Microtubule behavior during guidance of pioneer neuron growth cones in situ. *J. Cell Biol.* 115:381–395.
Schuch, U., M. J. Lohse, and M. Schachner. 1989. Neural cell adhesion molecules influence second messenger systems. *Neuron.* 3:13–20.
Singer, M. A., M. Hortsch, C. S. Goodman, and D. Bentley. 1992. Annulin, a protein expressed at limb segment boundaries in the grasshopper embryo, is homologous to protein cross-linking transglutaminases. *Dev. Biol.* 154: 143–159.
Smith, S. J. 1988. Neuronal cytomechanics: The actin-based motility of growth cones. *Science (Wash. DC).* 242:708–714.
Southwick, F. S., G. A. Dabiri, M. Paschetto, and S. Zigmond. 1989. Polymorphonuclear leukocyte adherence induces actin polymerization by a transduction pathway which differs from that used by chemoattractants. *J. Cell Biol.* 109:1561–1569.
Stossel, T. P. 1993. On the crawling of animal cells. *Science (Wash. DC).* 260:1086–1094.
Theriot, J. A., and T. J. Mitchison. 1992. Comparison of actin and cell surface dynamics in motile fibroblasts. *J. Cell Biol.* 119:367–377.
Theriot, J. A., and T. J. Mitchison. 1992. The nucleation-release model of actin filament dynamics in cell motility. *Trends Cell Biol.* 2:219–222.
Theriot, J. A., T. J. Mitchison, L. G. Tilney, and D. A. Portnoy. 1992. The rate of actin-based motility of intracellular *Listeria monocytogenes* equals the rate of actin polymerization. *Nature (Lond.).* 357:257–260.
Wang, Y.-L. 1985. Exchange of actin subunits at the leading edge of living fibroblasts: possible role of treadmilling. *J. Cell Biol.* 101:597–602.
Wang. L., and J. L. Denburg. 1992. A role for proteoglycans in the guidance of a subset of pioneer axons in cultured embryos of the cockroach. *Neuron.* 8:701–714.
Wang, N., J. P. Butler, and D. E. Ingber. 1993. Mechanotransduction across the cell surface and through the cytoskeleton. *Science (Wash. DC).* 260:1124–1127.
Williams, E. J., P. Doherty, G. Turner, R. A. Reid, J. J. Hemperly, and F. S. Walsh. 1993. Calcium influx into neurons can solely account for cell contact-dependent neurite outgrowth stimulated by transfected L1. *J. Cell Biol.* 119:883–892.
Yumura, S., and T. Kitanishi-Yumura. 1992. Release of myosin II from the membrane-cytoskeleton for *Dictyostelium discoideum* mediated by heavy-chain phosphorylation at the foci within the cortical actin network. *J. Cell Biol.* 117:1231–1239.
Zigmond, S. H., R. Furukawa, and M. Fechheimer. 1992. Inhibition of actin filament depolymerization by the *Dictyostelium* 30,000 D actin-bundling protein. *J. Cell Biol.* 119:559–567.